IJME

Int. J. of Applied Mechanics and Engineering, 2026, vol.???, No.???, pp.???-???
DOI: 10.59441/ijame/221376

INFLUENCE OF LOAD DISTRIBUTION PROFILES ON STRESS FIELDS AND STIFFNESS MODULUS UNCERTAINTY IN INDIRECT TENSILE TESTS: A FINITE ELEMENT ANALYSIS

H. Mezouara[1], M. Fahad[2], H. Zniker[3,4], E.M. Echebba[4], J. Zimou[1] and I. Feddal[5*]
[1]Laboratory of Material Physics and Subatomic, Faculty of Sciences,
Ibn Tofaîl University, MOROCCO
[2]Department of Transport Infrastructure and Water Resources Engineering,
Széchenyi István University, 9026 Gyor, HUNGARY
[3]International University of Casablanca,
Laboratory of Mathematics and Engineering Sciences, MOROCCO
[4]Civil and Environmental Engineering Laboratory (LGCE), Mohammadia Engineering School,
Mohammed V University, MOROCCO
[5]Optics, Materials and Systems Team, FS Abdelmalk Essaadi University, MOROCCO
E-mail: hichammezouara@gmail.com

The precise characterization of mechanical properties is essential to ensure the durability and safety of civil engineering infrastructures, particularly pavements. However, indirect tensile tests (IT-CY) on cylindrical specimens are sensitive to uncertainties related to non-uniform load distributions at the specimen–platen interface, which strongly influence the stress fields and the measurement of the stiffness modulus. This study employs finite element modeling (FEM) using the Abaqus software under the assumption of linear elastic behavior to analyze the impact of three load distribution profiles–uniform, sinusoidal, and parabolic–on the radial, tangential, and shear stress components in cylindrical specimens subjected to diametral compression, with a fixed contact angle of *15°*. The simulations reveal significant variations: the uniform distribution generates high stress concentrations (up to *40 MPa* in radial stress near the contact zones) and pronounced heterogeneity, thereby influencing the determination of the material's stiffness modulus. In contrast, the sinusoidal and parabolic profiles promote a smoother stress transition, reducing peak stresses by up to *60%* and concentrating the stresses along the vertical diameter. A comparative analysis with experimental results from previous studies supports these observations. Overall, the findings emphasize the critical role of contact conditions in minimizing experimental artifacts and reducing uncertainty in stiffness modulus evaluation. While based on a linear elastic framework, the results provide general mechanical insights that may contribute to the optimization of indirect tensile test protocols and the improvement of pavement design methodologies.

Key words: indirect tensile test; asphalt mixtures; load distribution; finite element analysis; stiffness modulus; measurement uncertainty.

1. Introduction

The precise characterization of the mechanical properties of materials constitutes a fundamental prerequisite to guarantee the reliability and safety of designs across all engineering disciplines. It also holds particular importance in the evaluation of stability and the estimation of the lifespan of infrastructures such as pavements, slopes, dams, or tunnels. In this context, the rigorous measurement of uniaxial compressive strength remains a key parameter to ensure the durability and safety of engineering projects, although its relevance, as an intrinsic property of the material or a simple design indicator, is still the subject of debates within the scientific community.

* To whom correspondence should be addressed

The most commonly used test is the indirect tensile test on cylindrical specimens, which consists of compressing the sample between two platens [1].

To ensure the reliability and repeatability of indirect tensile testing on cylindrical specimens, several standards have been developed, such as ASTM C39/39M-21 [2], ASTM D7012-23 [3], and ASTM D4543-19 [4]. Current test protocols defined by these standards primarily focus on dimensional tolerances and the flatness of loading platens. However, these standards rely on equations derived from simplified loading models that assume uniform radial pressure over a constant contact area. This approach neglects the phenomenon of progressive contact (advancing contact), in which the relative stiffness of the platens and the specimen continuously modifies the load distribution profile. Consequently, neglecting these variations in the stress and displacement fields may introduce significant bias in the evaluation of mechanical properties.

The results of tests aimed at determining the stiffness modulus can be influenced by various factors, such as the geometric characteristics of the tested sample [5, 6] or the instruments used to record relevant data [7]. These sources of influence contribute to increasing the measurement error during the evaluation of the stiffness modulus, particularly because researchers must make decisions with respect to the presence and distribution of natural heterogeneities within the material, as well as the contact conditions [7].
According to the existing literature, the interaction between the specimen and the press platens is decisive in generating the shear stress field near the contact zone [7].

To investigate the impact of the elastic properties of the platens on the distribution of contact stresses generated during the measurement of the stiffness modulus and on the associated error, a detailed analysis was conducted focusing on the effect of non-uniform loads and their impact on the different stresses, the measurement of the stiffness modulus, and the corresponding uncertainty. However, Real specimens systematically display geometric deviations from the ideal cylindrical shape, which are likely to affect the final contact configuration and, consequently, the stress distribution.

Mechanical properties constitute fundamental reference parameters in civil engineering, particularly for the construction and maintenance of road infrastructures. Their mechanical performance must be characterized with precision, especially when it comes to critical applications where the safety, durability, and longevity of structures are decisive. To ensure this rigorous evaluation, numerous European and international standards have been established. For example, the standard EN 12697-26 (2020) [8], entitled "Test Methods for Bituminous Mixtures – Part 26: Stiffness modulus", defines standardized protocols for measuring the stiffness modulus, a key parameter reflecting the material's ability to resist deformations under stress. This standard recommends the use of various test methods, among which the indirect tensile test for determining the stiffness modulus (ITSM) holds a prominent place. This test integrates factors such as temperature, loading frequency, and the type of applied stress, with displacement measurement performed via sensors placed on the loading platens, thus ensuring a reliable estimation of the actual deformation of the specime [9].

In recent years, indirect tensile testing of the material has been widely adopted for the evaluation and design of pavements [10, 11, 12, 13]. Among these methods, the indirect tensile test on cylindrical specimens (IT-CY) represents a reference approach for determination of the stiffness of the material. Applicable to cylindrical specimens of various diameters and thicknesses, whether prepared in the laboratory or extracted by coring from a pavement layer, this technique enables the analysis of the mechanical properties of bituminous materials, providing input parameters for pavement design and allowing the estimation of cracking resistance as well as pavement lifespan [14, 15, 16, 17, 18].

In the scientific literature, several studies have evaluated the mechanical properties of the material, focusing particularly on the measurement of the stiffness modulus. However, the results obtained often show significant variations, largely due to experimental artifacts inherent to the Indirect Tensile Stiffness Modulus (ITSM) test. These artifacts compromise the accuracy of the stiffness modulus measurements and can be summarized as follows:

1. Machine compliance in testing: This causes an overestimation of the specimen's deformation when the measurement relies on the crosshead displacement of the apparatus.
2. Friction between the sample and the loading platens: This phenomenon limits the Poisson's effect at the ends of the sample and causes localized bulging.

3. Misalignment of the loading platens or deformation of the sample ends: This generates a non-uniform load distribution, inducing substantial errors in the deformation measurement via LVDT sensors (Linear Variable Differential Transformers).
4. Localized crushing of the sample: It restricts the overall deformation and introduces significant biases in the results; such a failure must be identified to consider only pre-failure data during material characterization.

The accumulation of these influencing factors generally leads to systematic errors in the measurements for the stiffness modulus and Poisson's ratio, particularly an overestimation of the deformation and, consequently, an underestimation of the stiffness modulus. These inaccuracies highlight the need for refined metrology, particularly regarding the play in the loading platens and the non-uniformity of the platen-specimen contact, which are at the heart of the present research [19].

Efforts have been deployed to mitigate these problems in similar contexts, such as tests on foam-type materials. For example, [20] have demonstrated that deformations calculated from the crosshead displacement can lead to errors of *20* to *40%* on the Young's modulus. To correct the misalignment of the platens, the use of four extensometers has proven effective, although this approach is not systematically adopted in recent works. Other methods, based on direct and non-contact measurements of deformation, have been explored for the characterization of porous materials such as fiber-reinforced polyurethane foams. Among them, digital image correlation (DIC) techniques allow for obtaining reliable data by minimizing measurement errors, while providing precise information for numerical modeling and explaining the variability observed in the literature [21, 22]. These approaches have been motivated by the quest for precision in mechanical properties. However, although [20] rigorously examined the deformation measurement, they did not address Poisson's ratio nor the heterogeneity of stress and deformation through the thickness of the sample, particularly for thick samples. Moreover, DIC, although rich in data on surface displacements, presents limitations: The accuracy of the method critically depends on the quality of the speckle pattern applied to the specimen and it is less effective for structures without a natural pattern that is easy to track.

In the context of this study, these limitations in the literature motivate the use of numerical simulations to quantify the impact of the non-uniformity of the applied load on the propagation of radial and vertical contacts, and by extension on the measurement errors of the stiffness modulus of the material. This approach allows for optimizing test protocols and improving the reliability of mechanical evaluations.

Strain sensors such as LVDTs present certain limitations. Indeed, they can slip on the surface of the sample, which tends to underestimate the actual deformation. Moreover, their direct contact with the specimen can alter the mechanical behavior of the material, thus contributing significantly to the uncertainty of the stiffness modulus measurements [21].

Furthermore, numerous studies have focused on the influence of the contact pressure distribution on the propagation of stresses in the cylindrical specimen subjected to an indirect tensile test (Brazilian test). [23], using the complex potential functions method, examined different non-uniform distributions (parabolic and sinusoidal) and showed that the non-uniformity assumption significantly modifies the stress field, whether the distribution is point, uniform, parabolic, or sinusoidal. For their part, [24] studied the stresses generated by friction at the contact between the loading platen and the specimen. More recently, [25] conducted a numerical analysis of the stress distribution in the proximity of the interface under two contact conditions. They demonstrated that the formulas for calculating deformation and the stiffness modulus (E) derive directly from the stress and displacement solutions, which are themselves highly sensitive to the pressure distribution and friction. Thus, even for identical resultant forces, different contact distributions can generate notable discrepancies in the evaluation of stresses and the stiffness modulus. This underscores the need to study in depth the impact of loading conditions on the reliability of experimental results and on the measurement of the stiffness modulus of the material.

In the field of mechanical testing, it is widely accepted that the accuracy of the stiffness modulus evaluation depends closely on the loading conditions as well as the sensitivity of the measuring instruments. Several studies have particularly shown that, at low forces and small elongations, the uncertainty in determining the stiffness modulus increases, mainly due to the limitations and imperfections of the measuring devices used [26].

The works of [27] have revealed that classical models based on concentrated loads tend to overestimate the tensile stress maximum at the disk's center, particularly for materials with low stiffness modulus. In contrast, distributed contact models, which are closer to reality, provide estimates that better reflect the observed mechanical behavior, thus highlighting the importance of considering both the contact effect and the material's stiffness in the interpretation of indirect tensile tests on cylindrical specimens. Furthermore, numerical simulations performed using MATLAB show that the deformability of the sample, the curvature of the disk, as well as the characteristics of the loading platens, significantly affect the distribution of normal stresses, as well as the tensile and compressive stresses along the specimen's diameter.

The contact conditions between the loading platen and the cylindrical specimen play a determining role in the indirect tensile test (Brazilian test). Several studies have shown that the measured tensile strength increases with the central angle of the loading platen $\left(2\omega_0\right)$ [13-18-28] and that, When this angle is too small, the contact zone experiences a significantly higher pressure. Conversely, an increase in the contact angle tends in order to reduce the tensile stress at the center of the disk's end face, with the 15° angle being identified as ensuring the initiation of a central crack [29]. Moreover, contact conditions constitute the primary factor influencing the internal stress state [29, 30], while the evolution of the stress state and the fracture process under different arc loading angles has been analyzed [31, 32]. These works converge on the idea that the load distribution and contact angle affect not only the stress state and fracture mode, but also the variability of stiffness modulus tests and, consequently, the increase in uncertainty in experimental measurements. The assumption of uniform radial stress distribution is unrealistic; an analytical solution incorporating different loading schemes shows that when the curvature of the platens approaches that of the disk $\left(R_j = R\right)$, the biaxiality of stresses at the center deviates from theoretical values, rendering classical equations unsuitable [23-33]. The friction effect appears negligible at the center of the disk but remains significant in direct contact zones, influencing both the location and mode of fracture [30-34].

Accurate measurement of Poisson's ratio is a major challenge for reliable evaluation of material behavior. Previous works have shown that measured values of this coefficient are systematically higher at the center of the specimen faces, whereas its internal variation should theoretically remain low within the same sample. This phenomenon is mainly explained by friction effects between the contact surfaces and the machine's loading platens, which limit transverse deformation at the ends of the sample. By averaging front-back measurements, it has been observed that values recorded at the top and base generally converge with a discrepancy of less than 10%, indicating that the assumption of fully constrained transverse displacement leads to an overestimation of the effective stress. These observations suggest that some slippage at the specimen/platen interface must be taken into account to improve the representativeness of stiffness measurements [21].

The present analytical study has also confirmed that considering an advanced contact the interaction between the cylindrical specimen and the loading platens results in a non-linear increase of the applied load with respect to platen displacement [35].

Several studies have emphasized that experimental validation remains a major challenge due to uncertainties related to measurements and experimental conditions that are often difficult to control. In this context, numerical simulations provide a relevant alternative. As reported in the literature [32-34-36, 37], finite element models allow for precise reproduction of the behavior observed during the Brazilian test.

This study presents a comprehensive analysis of finite element models representing various test configurations. The study highlights the effect of the non-uniform distribution of the load applied by the loading platens on the propagation of stresses in the cylindrical specimen and on the uncertainty of stiffness modulus measurements for of the material.

According to [21], several experimental factors can compromise the accuracy of deformation measurements during mechanical tests. Among these are the compliance of the testing machine, friction at the interfaces between platens and sample, misalignment of contact surfaces, as well as localized crushing of the specimen. To limit this latter effect, the authors deliberately applied load levels below the material's elastic limit. Nevertheless, the other experimental artifacts continued to influence the results.

In particular, the compliance of the machine has been identified as a major cause of repeatability errors, resulting in an underestimation of the stiffness modulus when deformation is deduced from the crosshead displacement. Furthermore, misalignment of the platens constitutes another significant source of artifacts. Using optical tracking (OT), Marter *et al.* [21] were able to map the evolution of deformations across different zones of the sample and highlight local heterogeneities in the stress-strain behavior, linked to non-uniform loading. The study showed that certain zones exhibited an initially non-linear response, while others displayed a delay in load transmission, indicating lateral imbalance. By averaging front/back measurements, the effects of misalignment and out-of-plane movements could be reduced, allowing for a more homogeneous response. However, significant discrepancies in maximum deformation values persisted depending on the measurement location, leading to notable variations in Young's modulus in different directions.

On their side, [38] showed that radial and shear stresses are particularly sensitive to the geometry of the applied load distribution, while circumferential stresses exhibit more localized variations, primarily in the contact zone and along the vertical axis of the disk. The authors emphasize that the assumption of a uniform distribution, although theoretically simple, tends to induce excessive deformations in soft materials, thereby limiting its relevance in this context. Their approach relies on the assumption of concentrated radial loads applied along a diameter, which neglects tangential shear stresses at the boundary. However, in real experimental conditions, parameters such as contact friction or the relative stiffness of the materials (sample/platen) have a crucial role in the effective distribution of shear stresses. These effects influence not only the actual shape of the contact distribution but also the location of fracture initiation.

Several recent studies have revisited the Brazilian test through contact mechanics. Thus, [30] proposed modeling this test as a Hertzian contact problem, taking into account the geometry of the loading platens. The latter directly conditions the internal stress state of the disk and leads to a circular distribution of the load along the contact crown. However, such a distribution escapes treatment by the classical method of complex potentials.

In extension, [33] deepened the study of mechanical contact between a cylindrical specimen and loading platens subjected to non-uniform distributions, this time resorting to Muskhelishvili's complex potentials method. Their analysis aimed to quantify and interpret stress fields as a function of the curvature ratio r, defined as the ratio of the curvature of the specimen and that of the platens. This approach highlighted the combined influence of the platens' geometry and the relative stiffness of the materials (specimen and platens) on the stress distribution in the sample.

Furthermore, recent research emphasizes that the location of the fracture initiation point in the Brazilian test strongly depends on the contact angle between the disk and the loading jaws [39]. It has been shown that the larger this angle, the closer the cracking initiates to the center of the disk, independent of the type of applied radial distribution (uniform or sinusoidal), the chosen fracture criterion, or the material studied. In contrast, frictional stresses at the specimen-platen interface exert limited influence on the initiation process.

In summary, experimental conditions and geometric variations of the samples generate non-uniform stress and strain states, making the interpretation of the test more complex and dependent on contact parameters. This research therefore aims to analyze, via numerical simulations and a metrological approach, the impact of mechanical play in the loading platens and non-uniformity of contacts on the measurement of the stiffness modulus of the material, to improve the reliability and repeatability of the tests.

2. Approach to the method

2.1. Preliminary aspects

The geometry of the testing apparatus, along with the configuration of the loading strips, are critical parameters influencing the mechanical behavior of specimens tested using the indirect tensile test (Fig.1). The work of [37] demonstrated that crack initiation most frequently occurs within the contact zones between the loading strip and the cylindrical specimen. This localization is explained by the singularity of the stress and strain field generated by the strip configuration, which induces significantly higher stress concentrations than those observed at the disk center. Such heterogeneity alters the internal stress distribution within the sample and can compromise the reliability of the results if the contact geometry is not strictly controlled.

A primary challenge in the indirect tensile test on cylindrical specimens is the development of high-stress fields near the contact zones between the loading strips and the specimen. These localized stress concentrations complicate the interpretation of results and can introduce bias in the evaluation of mechanical properties. For this reason, numerous experimental and theoretical studies conducted over several decades have focused on proposing approaches to mitigate these effects and enhance the test's reliability.

In the context of evaluating the stiffness modulus of asphalt mixtures using the indirect tensile test on cylindrical specimens, this study adopts a metrological approach to examine the effect of mechanical play in the loading strips on the stress distribution within the sample. The analysis also investigates the influence of these parameters on measurement uncertainty, result variability, and, more broadly, on the reliability and overall quality of the tests.

The bituminous mixture is modeled using a linear elastic isotropic constitutive law with Young's modulus and Poisson's ratio values representative of typical asphalt concretes under the simulated loading conditions. While this assumption neglects the viscoelastic nature of the material, it is justified for the purpose of this parametric study, which aims to highlight the relative impact of load distribution profiles on stress heterogeneity and modulus estimation uncertainty.

In general, previous research has focused on optimizing experimental conditions and measurement protocols for asphalt mixture stiffness tests. Particular attention has been given to the contact geometry between the loading strips and the specimen, as well as to the consideration of the elastic properties of the two interacting bodies [23-30].

Mechanical play between the loading strips and the specimen, combined with various geometric and physical imperfections, can induce significant perturbations in stress propagation, thereby reducing the representativeness and reliability of experimental results. Among the frequently reported imperfections are:

- The surface roughness of the specimen (Fig.2),
- Irregularity or non-uniformity of the lateral faces,
- Misalignment of the specimen within the device,
- Ovalization or slight eccentricity of the cross-section (Fig.3),
- As well as wear of the strips or poor pressure distribution in the contact zones.

The contact zone between the loading strip and the specimen may take two main geometric configurations:

- A conforming contact, corresponding to a curved section that follows the natural lateral surface of the right circular cylinder,
- Or a non-conforming contact, resulting from a flat portion obtained by locally flattening the cylinder's surface [40].

These contact conditions directly influence load transfer, the localization of maximum stresses, and the mechanisms of crack initiation and propagation. Their analysis from a metrological perspective is therefore essential for identifying sources of uncertainty and ensuring the traceability, repeatability, and robustness of stiffness tests for asphalt materials.

The mode of load application on a cylindrical specimen during indirect tensile tests directly influences the stress distribution within the material. Although transmitted by the loading strips, this load can be assumed to be uniform over the contact area, but in practice, it is often non-uniform (as illustrated in Fig.1b). Depending on the experimental conditions and strip geometry, the applied pressure can adopt various profiles, such as parabolic or sinusoidal distributions, thereby significantly altering the localization and intensity of the maximum stresses.

Furthermore, the direction of the load applied to the specimen varies depending on the device configuration. It can be oriented parallel to the specimen's axis or radially towards its geometric center. This orientation directly influences the lateral deformations recorded by LVDT sensors, thus impacting the accuracy and reliability of the stiffness modulus measurement.

In the specific case of Hertzian contact, as described by [23-30], the contact area is limited to a point or a line, under the assumption that both bodies behave elastically and that no cohesion exists between them. The exerted pressure can be distributed according to various radial profiles–uniform, parabolic, or sinusoidal. These distributions are strongly influenced by the mechanical properties of the contacting materials, notably

by Young's modulus and Poisson's ratio, as well as by the local geometry of the contact zone, including curvature, roughness, and flatness.

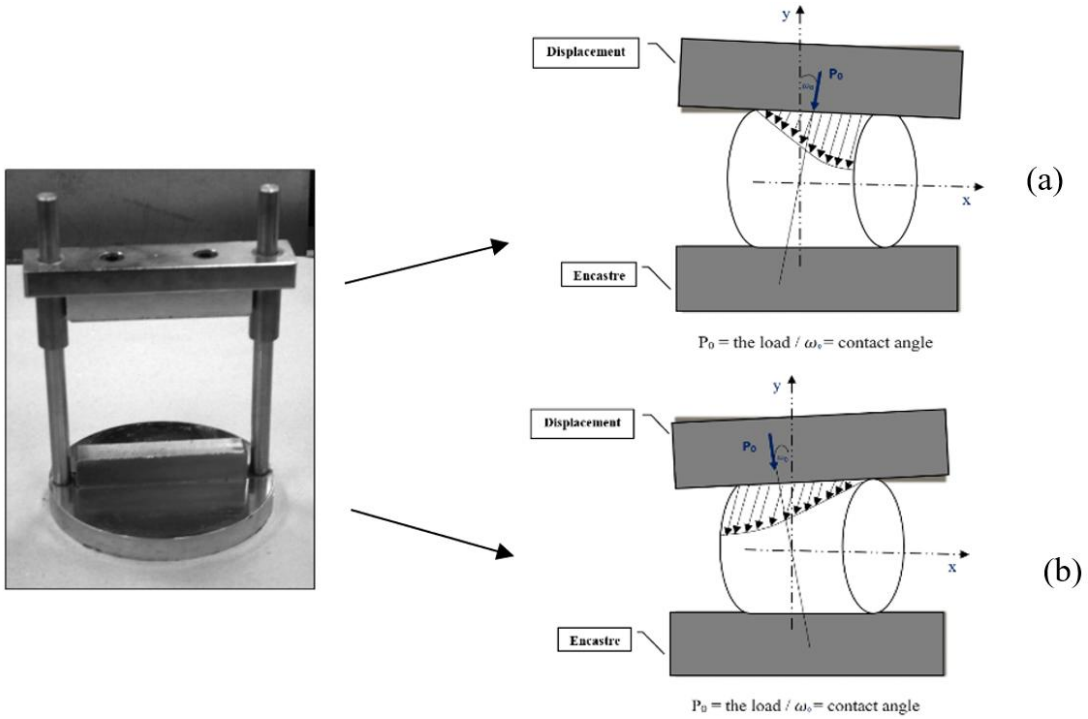

Fig.1. Photograph of a Typical Indirect Tensile Test (IDT) Loading Fixture, (a), (b) Non-uniform loading.

Fig.2. Surface Roughness Defects on a Cylindrical Test Specimen.

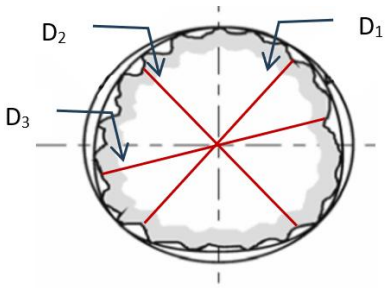

Fig.3. Circularity Defect on a Cylindrical Test Specimen (Variable diameter along the specimen: $D_1 \neq D_2 \neq D_3$).

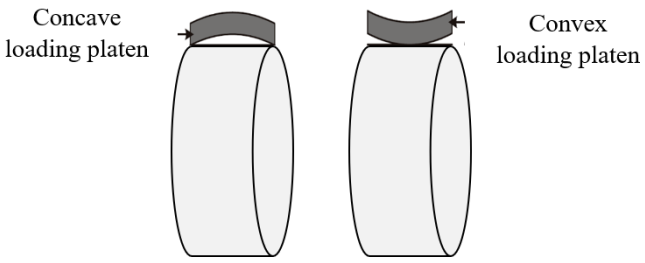

Fig.4. Platen flatness deviations.

Thus, any variation in the contact conditions or load distribution can generate significant uncertainty in the experimental results, particularly when estimating the stiffness modulus of asphalt mixtures. The rigorous control of these parameters is therefore essential to ensure the reliability, repeatability, and traceability of measurements obtained during mechanical characterization tests.

The hardness and flatness of the steel platens used in compression testing are factors that can influence the reliability of the results. In particular, when a platen deforms under load, adopting a concave shape, the distribution of forces becomes more concentrated at the center of the specimen, leading to a distortion of the measurements (Fig.4). This type of defect generally occurs when the thickness of the platens is insufficient or when their dimensions are smaller than those of the specimen.

2.2. Load distributions considered

The load distribution profiles selected for this study–uniform, sinusoidal, and parabolic–are intended to represent the interaction between the specimen and the loading jaws within the framework of elastic contact mechanics and correspond to theoretical models commonly adopted in Brazilian test analyses.

The uniform distribution serves as a classical reference case, although it may generate stress discontinuities at the contact edges. In contrast, the sinusoidal and parabolic profiles provide a smooth stress transition along the loaded arc, in accordance with contact mechanics principles first introduced by Heinrich Hertz and later formalized in plane elasticity by Nikolai Muskhelishvili.

From a metrological perspective, the goal is not to reproduce a specific experimental configuration, but to evaluate the sensitivity of the stress field and stiffness modulus estimation to contact assumptions. As shown by Diego José Guerrero-Miguel *et al.* (2019) [23], the actual pressure distribution directly affects the internal stress state and the resulting mechanical properties.

Mathematically, these three load distributions are described by Eqs (2.1) to (2.3) [30-35], respectively. Their selection allows the representation of different boundary contact conditions and provides a controlled framework to account for effects such as geometric misalignment in the loading apparatus and variations in support due to clearance in the compression platens.

These distributions are implemented in a numerical simulation environment using Abaqus to evaluate their influence on stress distribution and stiffness modulus of asphalt mixtures under indirect tensile testing of cylindrical specimens. This approach focuses on quantifying the sensitivity of the mechanical response to the assumed contact model rather than reproducing an exact experimental pressure profile.

$$P_{uniform}(\alpha)=\frac{P}{2R\omega_0}, \tag{2.1}$$

$$P_{parabolic}(\alpha)=\sqrt{\frac{3\pi P}{32kR}}\left(1-\frac{\sin^2(\alpha)}{\sin^2(\omega_0)}\right), \tag{2.2}$$

$$P_{sinusoidal}(\alpha)=\frac{P(\cos\alpha-\cos\omega_0)}{2R(\sin\omega_0-\omega_0\cos\omega_0)}. \tag{2.3}$$

Where:

- R is the radius of the disc,
- P represents the total applied load, equivalent to that in the concentrated load scenario.
- α represents the rotation angle from the vertical diameter to the line of action of the load,
- ω_0 represents the contact angle between the loading jaw and the specimen,
- $P_0 = P/w$ is the normalized load, obtained by dividing the total load by t specimen's thickness w.
- k depends on Muskhelishvili's constants, used in analytical solutions for plane stress conditions.

Maximum load in the distribution is expressed as a function of P_0. Under the aforementioned boundary conditions, and considering the resultant force P_0 (i.e., the total external load P divided by the thickness w), the stress distribution can be more precisely evaluated along the contact zone.

It is important to note that the uniform distribution is constant, being independent of the angle α. Nevertheless, it is expressed as $P(\alpha)$ since it represents the stress along the loaded boundary zone.

When considering the elastic contact between the two bodies, the parameters P (applied load) and ω_0 (contact angle) are no longer independent.

While the parabolic load distribution is of special interest because it accounts for the elastic properties of both the jaw and the specimen, it yields results similar to the sinusoidal case for an identical contact angle [23].

For the maximum value (reached at $\alpha = 90°$), the expressions associated with the normalized load P_0 are defined for the uniform, parabolic, and sinusoidal distributions. These distributions are described by the following Eqs (2.4) to (2.6), [30-35].

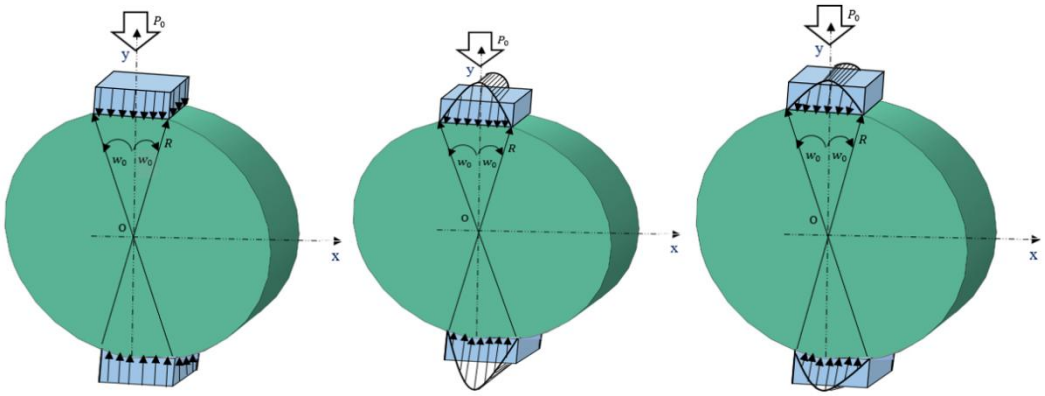

5. Schematic representation of the loading types applied to the cylindrical specimen: (a) uniform distribution, (b) parabolic distribution, (c) sinusoidal distribution.

$$P_{uniform}=\frac{P_0}{2R\omega_0}, \tag{2.4}$$

$$P_{parabolic}=\sqrt{\frac{3\pi P_0}{32kR}}, \tag{2.5}$$

$$P_{sinusoidal} = \frac{P_0\left(1-\cos\omega_0\right)}{2R\left(\sin\omega_0 - \omega_0\cos\omega_0\right)} \,. \tag{2.6}$$

2.3. Numerical simulation

In this study, the objective is not to determine the precise stress distribution at the contact between the loading strips and the cylindrical specimen during the indirect tensile test, but rather to evaluate the impact of different load distribution hypotheses on the internal stress field within the sample. This analysis is particularly relevant for viscoelastic materials, such as asphalt mixtures, for which an accurate estimation of the stiffness modulus and a thorough understanding of stress transfer mechanisms are essential.

The adopted approach is based on comparing three theoretical load distributions commonly found in the scientific literature: the uniform distribution, the parabolic distribution, and the sinusoidal distribution. These profiles aim to represent different contact conditions at the interface between the loading jaws and the specimen. This comparison thus enables a better understanding of the influence of boundary conditions, particularly the stress distribution shape across the contact zone, on the overall mechanical response of the material.

The selection of a fixed *15°* contact angle for all numerical simulations is based on a rigorous metrological compromise between fidelity to the theoretical model and the reduction of experimental artifacts. According to the work of Erarslan (2011) [32] and the analytical solutions developed by Hondros (1959), this angle represents the upper limit that ensures an error of less than *2%* in the calculation of tensile stresses at the center of the specimen compared with the classical Brazilian test formula.

Moreover, applying the load over a *15°* arc has been documented as sufficient to limit localized crushing phenomena at the contact points while producing a stress field representative of pure diametral compression. By fixing this parameter, the present study specifically isolates the influence of the loading profile morphology (uniform, sinusoidal, or parabolic) on the measurement uncertainty of the stiffness modulus, thereby strengthening the robustness of the comparative analysis of interface conditions.

Numerical modeling is implemented using the finite element analysis software Abaqus, which allows for the precise simulation of the stress fields associated with each distribution. This approach provides a robust analysis tool for studying the mechanical behavior of the specimen subjected to different loading configurations, integrating factors such as misalignment defects or platen play.

The simulations are conducted under strictly controlled conditions, maintaining:

- A constant specimen geometry,
- An identical total applied load,
- A fixed contact angle of $\omega_0 = 15°$.

The resulting stress fields are then normalized with respect to the maximum stress to enable a direct comparison between the different loading hypotheses.

A targeted analysis is subsequently conducted along two principal directions:

- The vertical radius, which traverses the contact zone with the strips,
- And the horizontal radius, perpendicular to the loading direction.

These directions are particularly sensitive to stress concentrations, making them reliable indicators for assessing the effect of load distributions on the specimen's behavior. This analysis highlights how the load distribution shape and the contact angle affect the local stress state, and consequently, the reliability of the Brazilian test for mechanically characterizing asphalt mixtures.

2.4. Finite element analysis of diametral compression loading

The geometry of the cylindrical specimen was modeled in a three-dimensional environment with Two compression platens placed on the top and bottom faces, in direct contact with the specimen surface. This configuration accurately replicates the conditions of the indirect tensile test performed experimentally (see Tab.1).

The simulation results closely matched the experimental data, indicating that the FE model can reliably predict the mechanical behavior of asphalt materials [15].

The input mechanical parameters used for the numerical simulation of the material were determined from laboratory tests. The yield stress limit of the asphalt mixture was evaluated at $\sigma_{-limit} \approx 0.028\ MPa$, based on experimental results obtained during stiffness modulus determination tests [19].

From the perspective of boundary conditions, the bottom platen was modeled as perfectly fixed, while a prescribed displacement of $\delta = 5\mu m$ was applied to the top platen along the vertical direction (*Y*-axis). Furthermore, the movement of the disc was restricted along the *X* and *Z* axes to reproduce the experimentally observed contact conditions, particularly by simulating the effect of support play or geometric misalignment. The numerical model was developed in ABAQUS using eight-node linear hexahedral elements (C3D8R), i.e., reduced-integration elements with enhanced hourglass control, to model the cylindrical specimen and the compression platens. This element type, widely employed in nonlinear analyses, is recognized for its numerical robustness and its ability to accurately capture high stress gradients.

To ensure the stability and reliability of the reported stress amplitudes, a rigorous mesh convergence study was conducted. A significant local mesh refinement was applied in the vicinity of the specimen–platen interface, a region characterized by high stress concentrations due to the abrupt transition associated with the uniform loading profile. Convergence was considered achieved when the maximum von Mises stress no longer varied significantly between two successive mesh refinements. The final converged model consisted of 29,492 elements.

Friction at the interface between the loading platens and the specimen is a well-known factor influencing stress fields, particularly by restricting the Poisson effect at the specimen ends and causing localized bulging [15-21]. Previous studies indicate that friction plays a crucial role in the effective distribution of shear stresses and can significantly influence the localization of crack initiation [30-39]. However, within the framework of the present numerical simulation, a perfectly sliding (frictionless) interface was adopted, in accordance with several reference analytical approaches. This methodological choice was motivated by the objective of isolating the intrinsic influence of the three load distribution profiles (uniform, sinusoidal, and parabolic) without interference from tangential stresses. Furthermore, the literature confirms that although friction effects are predominant in the immediate contact zones, they remain negligible at the center of the disk, which is the critical region for calculating the stiffness modulus and tensile stress [25-29-33, 34]. This assumption therefore ensures a direct and consistent comparison between the different radial pressure models investigated.

Table 1. Specimens's properties.

Diameter *D* (*mm*)	*100*
Thickness *t* (*mm*)	*53*
Forced displacement of δ (μ*m*)	*5*
Stiffness Modulus *E* (*MPa*)	*6683.75 ± 555.52*
Poisson's ratio ν	*0.35*

3. Results and discussion

3.1. Stress field across the entire specimen

To analyze the influence of different contact conditions at the interface between the loading platens and the cylindrical specimen with respect to the stress distribution, the stress fields were evaluated and compared for each principal component (radial, tangential, and shear). All stress fields were normalized with respect to their maximum value (in tension or compression), typically observed in the radial and tangential (hoop) stress components. Subsequently, a detailed analysis was conducted along the vertical and horizontal diameters of the specimen, these directions being particularly representative of critical zones in the context of the Brazilian test. The figures show the normalized stress components for a fixed contact angle.

3.2. Comparative analysis of the radial stress field under different loading distributions

Figure 6 illustrates the distribution of the normalized radial stress field (σρ) in a cylindrical specimen subjected to three types of load distributions: uniform (a), sinusoidal (b), and parabolic (c).
It emerges that the uniform distribution induces a more homogeneous stress state inside the sample. The radial field decreases progressively from the contact zones to the specimen center. However, local stress concentrations appear in the immediate vicinity of the contact zones, reflecting the abruptness of the transition between loaded and unloaded areas.

In contrast, distributions with smooth transitions, such as sinusoidal and parabolic forms, generate a more localized dissipation of stresses. The stress field is strongly concentrated along the vertical diameter, while the rest of the specimen remains relatively less stressed. This phenomenon is particularly visible in the parabolic configuration (c), which exhibits intermediate behavior between the two extremes.
In all cases, a tensile zone is observed at the specimen center. This zone is more pronounced in the case of non-smoothed distributions, in the region where the ratio of tensile to compressive stresses reaches its maximum.

Thus, loadings with progressive transitions allow for a reduction in stress peaks but concentrate the efforts more in limited regions. The relative differences between stress states can reach up to *25%*.

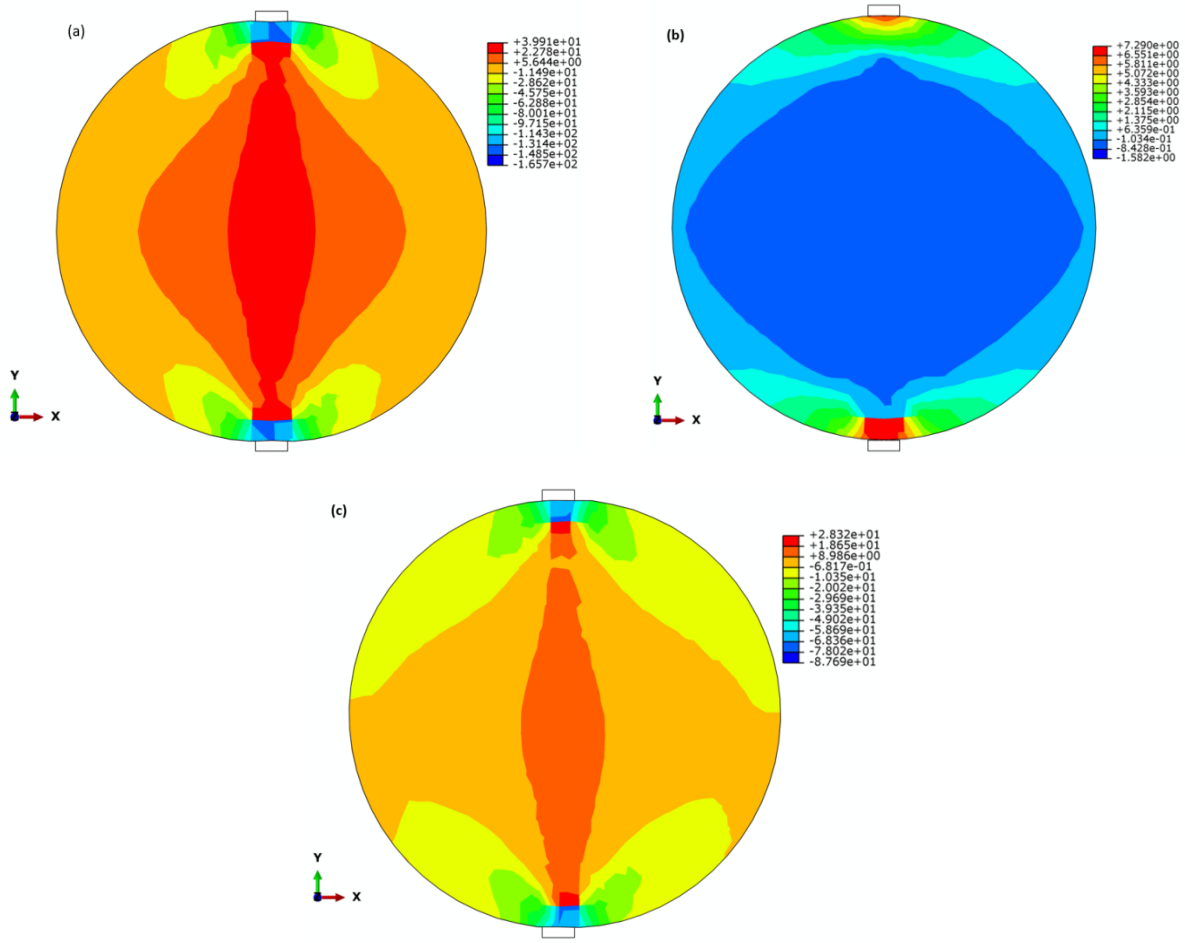

Fig.6. Normalised radial stress components in uniform (a), sinusoidal (b), and parabolic (c) distributions.

3.3. Comparative analysis of the tangential stress field (σθ) (hoop stress) under different loading distributions

Significant qualitative differences are observed in the contact zones between the platens and the specimen, highlighting the direct influence of the loading mode on the $\sigma\theta$ field behavior.

The uniform loading generates localized stress concentrations in the support zones, leading to a strong break in radial symmetry and marked heterogeneity of the field. These zones of intense compression can induce potential fragility points and crack initiations, particularly in quasi-brittle materials.

In contrast, the sinusoidal loading allows for a more regular and continuous distribution of tangential stresses. The variations are concentrated only around the contact points, while the rest of the disk remains subjected to low stress levels. This regularity significantly reduces local deviations, with variations nearly *60%* lower compared to uniform loading.

The parabolic loading presents an intermediate behavior. Although the stress range is comparable to that of uniform loading, the transitions are more progressive, resulting in a better distribution of mechanical efforts and an attenuation of local singularities. In areas away from the contact, the difference between the parabolic and sinusoidal fields is generally less than *10%*.

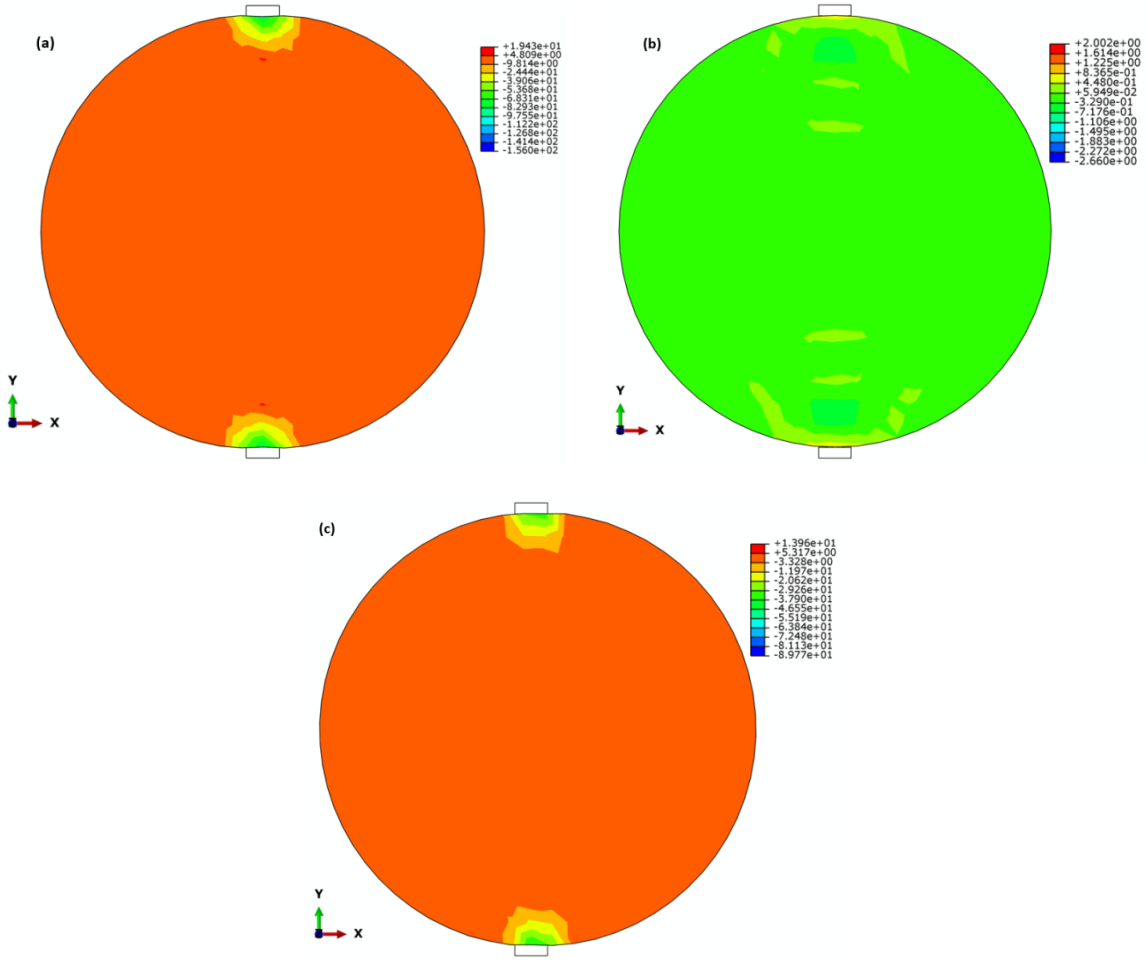

Fig.7. Normalised hoop stress components in uniform (a), sinusoidal (b), and parabolic (c) distributions.

3.4. Comparative analysis of the tangential stress field (τ_*r*θ) (hoop stress) under different loading distributions

Figure 8 presents the distribution of the shear stress field τ_*r*θ in a cylindrical specimen subjected to different load distributions, namely uniform, sinusoidal, and parabolic. Shear stresses are positive in the first and third quadrants, and negative in the second and fourth, indicating identical orientations but opposite directions.

The normalized values reveal that the maximum stresses reach about *20%* of the radial component for the uniform distribution, and up to *25%* for the sinusoidal and parabolic distributions, highlighting the favorable effect of these sinusoidal and parabolic distribution types on the stress distribution.

The shear peaks are concentrated at the periphery of the specimen and decrease towards the center, canceling out along the angular directions. The vertical and horizontal diameters correspond to the principal directions, where the shear is zero, regardless of the load distribution.

A localized shear appears near the center, attenuated by smoothing (sinusoidal and parabolic), demonstrating the direct impact of the load regularity on the formation and intensity of the shear field.

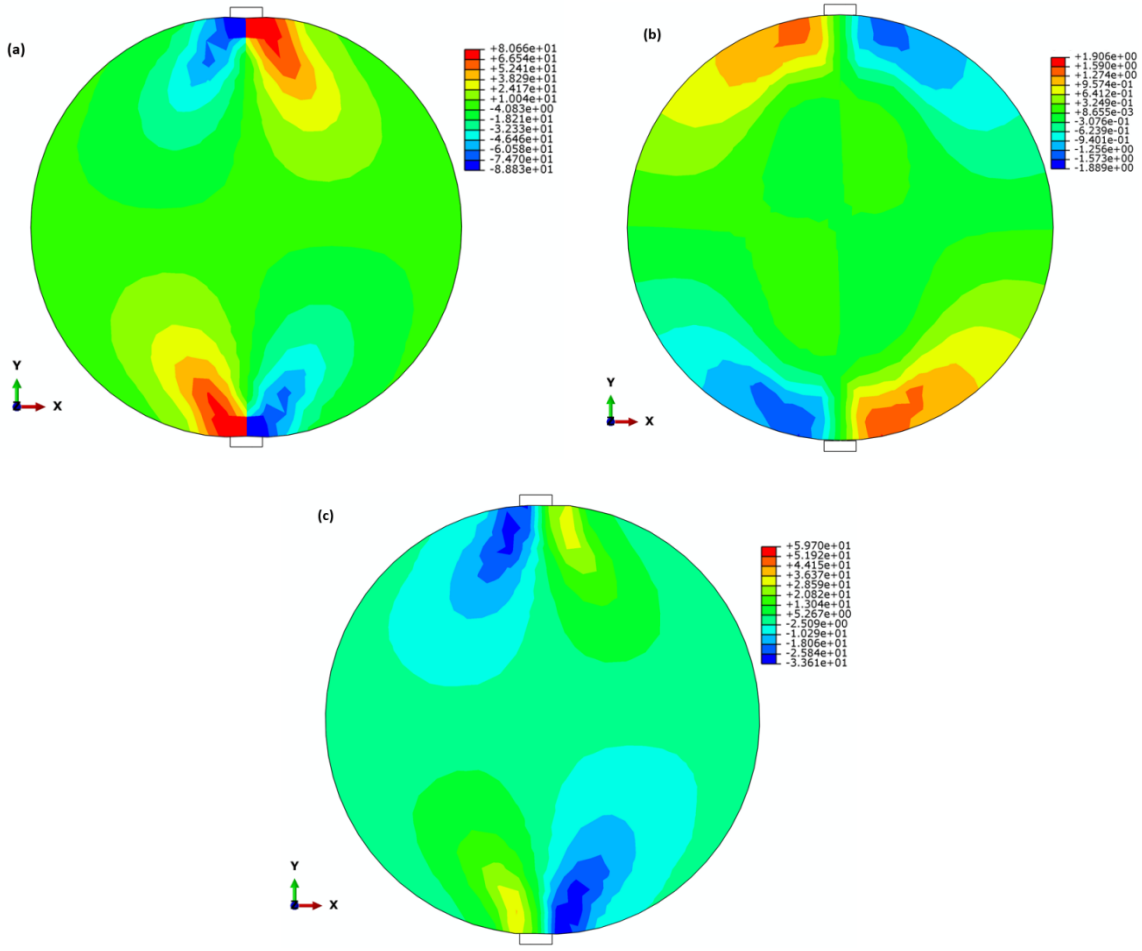

Fig.8. Normalised shear stress components for uniform (a), sinusoidal (b), and parabolic (c) distributions.

3.5. Differences among distributions

From a metrological perspective, the discrepancies between the stress distributions can be interpreted as an uncertainty associated with the modeling of the stress field, depending on the loading profile under

consideration. A comparative analysis of the radial and tangential components was conducted along the vertical and horizontal axes, allowing the evaluation of the stress field's sensitivity to different loading conditions.

Vertical radius

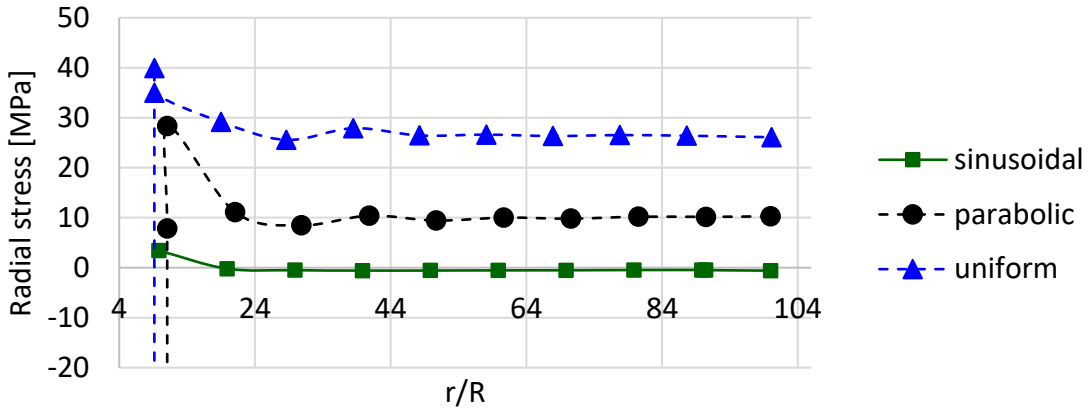

Fig.9. Normalised radial stress components for uniform, sinusoidal, and parabolic distributions along the vertical radius.

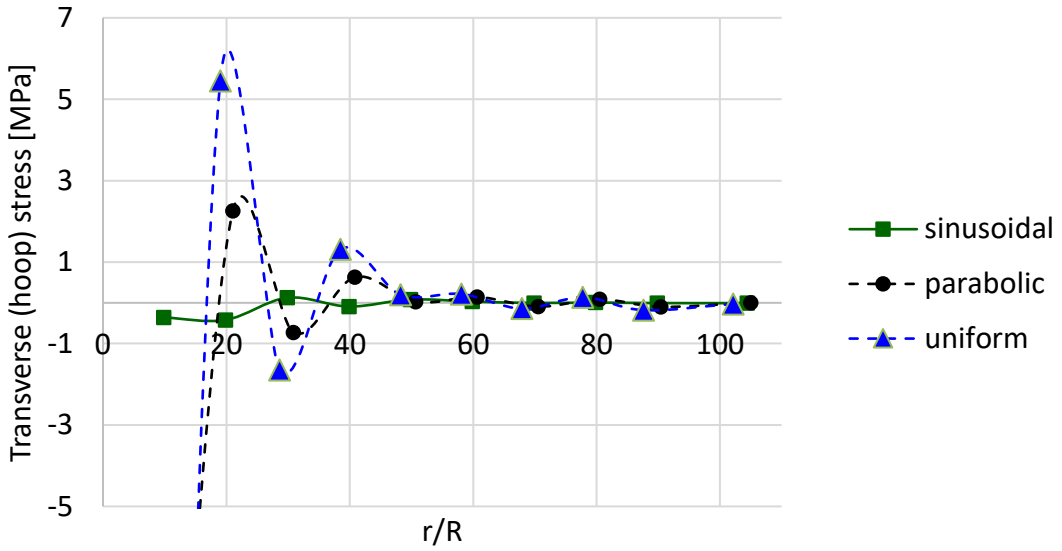

Fig.10. Normalised hoop stress components for uniform, sinusoidal, and parabolic distributions along the vertical radius.

Figure 9 shows the distribution of radial stresses as a function of the *r/R* ratio for three types of contact pressure distributions: sinusoidal, parabolic, and uniform. It is clearly observed that the radial stress varies significantly depending on the shape of the applied pressure. The uniform distribution generates the highest values near the contact area $(r / R \approx 4)$, with a peak reaching approximately *40 MPa*, followed by a gradual decrease to a plateau around *27 MPa*. This trend is typical of an abrupt pressure distribution, lacking a smooth transition at the contact edge, which leads to more pronounced stress concentrations.

In comparison, the parabolic distribution exhibits a smoother transition, with a lower initial stress (approximately *30 MPa*), but most notably a rapid drop to a nearly stable value of about *10 MPa* beyond $r/R = 24$. This evolution indicates a better distribution of the load over the contact surface, thereby reducing localized stress peaks. The sinusoidal curve, on the other hand, generates the lowest radial stresses across the entire domain. The values remain close to zero after $r/R \approx 10$, indicating a well-controlled compressive state without significant concentration.

Of particular interest are the differences between the distributions become negligible beyond $r/R > 60$, where the stresses tend to stabilize. However, in the area close to the contact $(r/R < 20)$, the discrepancies are significant, with potential errors exceeding 50% between the uniform distribution and the smooth transitions.

Figure 10 complements this analysis by showing the hoop stress components along the same vertical radius. It is observed that the uniform distribution also causes significant peaks, while the parabolic and sinusoidal profiles provide a more stable and better-distributed mechanical response.

Therefore, the nature of the contact pressure distribution has a direct influence on the generated stress states. Smooth transition profiles, such as parabolic and sinusoidal, help limit stress peaks, unlike the uniform distribution, which strongly accentuates them at the contact edge.

These stress variations can alter the local mechanical response and skew the evaluation of the stiffness modulus, leading to overestimation or underestimation, and an increase in measurement uncertainty.

Horizontal radius

Figures 11 and 12 present the normalized radial and hoop stress components along the horizontal radius, respectively. Unlike the observations made along the vertical radius (Figs 9 and 10), where significant discrepancies were noted between the different pressure profiles, the results along the horizontal axis show lower sensitivity to the type of distribution.

In Fig.11, the radial stress gradually decreases regardless of the profile, with notable differences only at very low *r/R* values. The uniform distribution remains the highest initially but quickly converges toward the values of the parabolic and sinusoidal profiles beyond $r/R \approx 100$. Figure 12 confirms this trend, with extremely low hoop stresses, on the order of *0.1 MPa*, and minimal differences between the curves.

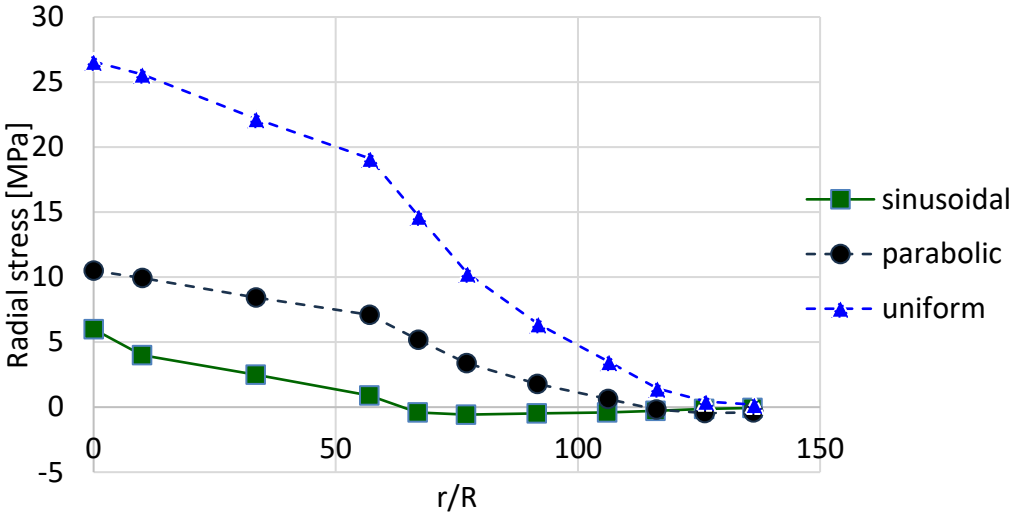

Fig.11. Normalised radial stress components for uniform, sinusoidal, and parabolic distributions along the horizontal radius.

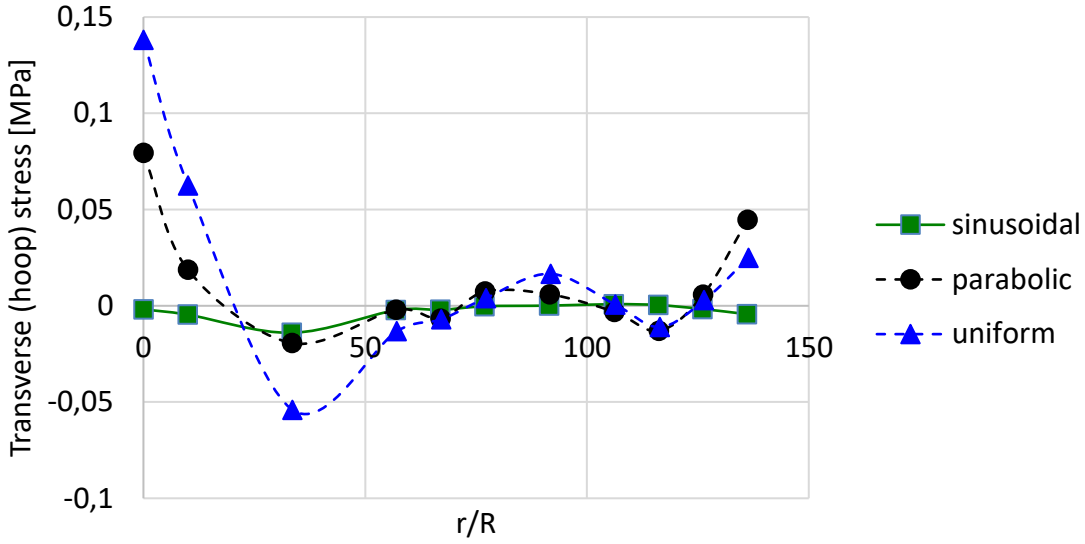

Fig.12. Normalised hoop stress components for uniform, sinusoidal, and parabolic distributions along the horizontal radius.

These results suggest that, unlike the vertical radius where stress concentrations are strongly influenced by the pressure profile, the stress field along the horizontal radius remains relatively insensitive to this variation. This anisotropic behavior can be explained by the contact geometry and the direction of the applied loads, which concentrate efforts primarily in the vertical direction.

3.6. Localized stress behavior at the disk–platen interface

In the context of analyzing the mechanical behavior of materials under the indirect tensile test on cylindrical specimens, Fig.13 shows the distribution of normalized stresses at the interface between the loading platens and the cylindrical specimen for three types of load distributions: uniform, sinusoidal, and parabolic. The objective of this study is to evaluate the impact of contact conditions on the intensity and localization of applied stresses, with a view to better understanding the induced effects on the measurement of material stiffness in indirect tension.

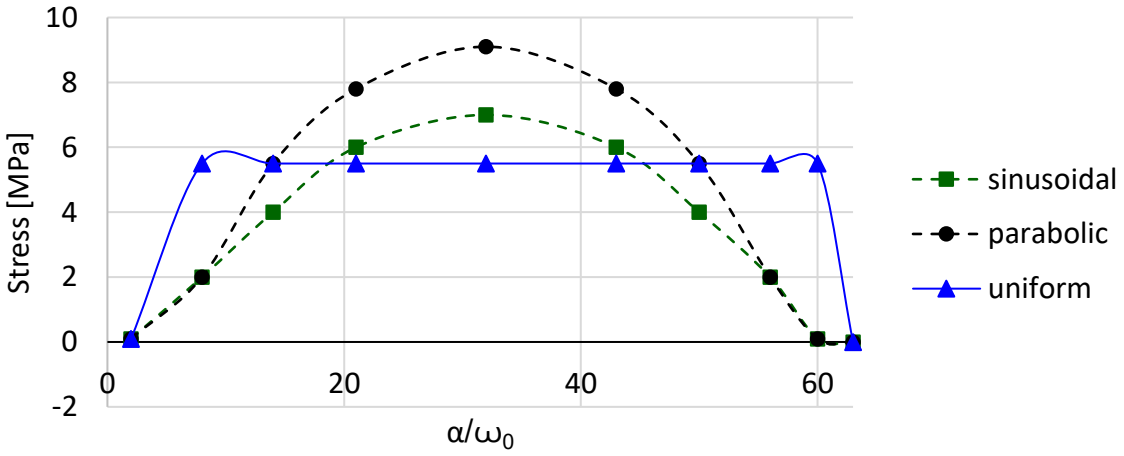

Fig.13. Local stress distribution at the disk-plateau interface for different loading profiles.

The analysis of the curves highlights significant discrepancies between the distributions. The parabolic configuration generates the highest maximum stress, reaching approximately *9 MPa*, representing a *30%* increase compared to the uniform distribution, which peaks at around *6 MPa*. The sinusoidal distribution, on its side, shows a maximum approaching *7 MPa*, or a *17%* discrepancy relative to the uniform distribution.
The parabolic distribution stands out due to a concentration of stresses at the center of the interface, reflecting a marked localization of applied forces. This concentration is likely to accentuate compression effects in the loading zone, which can have a direct influence on interpreting the material's behavior. In contrast, the uniform distribution induces a more constant spread along the interface.

These observations confirm that the choice of loading profile significantly influences the local stress distribution. Variations of up to *30%* between configurations show that the contact shape is not a neutral parameter. It must be rigorously defined and controlled to ensure the reliability and reproducibility of experimental measurements.

The numerical simulations conducted in this study demonstrate the profound impact of load distribution profiles on stress fields within cylindrical specimens of the material during indirect tensile tests (IT-CY). Uniform loading generates extensive stress heterogeneity, with radial peaks reaching up to *40 MPa* near contact zones and variations in circumferential stresses exceeding *60%* compared to smoother profiles (sinusoidal and parabolic). These concentrations result from abrupt transitions at the sample-platen interface, leading to localized deformations that can compromise the accuracy of stiffness modulus measurements. In contrast, parabolic and sinusoidal distributions facilitate progressive stress dissipation, confining high values to the vertical diameter and reducing overall peaks by *30* to *50%*, thereby promoting a more homogeneous internal response. Shear stresses, although secondary (*20* to *25%* of radial components), exhibit similar sensitivity, canceling out along principal directions but intensifying at the periphery under uniform conditions.

These observations align closely with analytical and numerical studies in the literature. For example, Markides and Kourkoulis [33] reported comparable discrepancies (up to *35%*) in tangential stresses for parabolic distributions at high contact angles, attributing them to curvature ratios between platens and samples. Similarly, Yuan and Shen [25] highlighted the role of friction and pressure non-uniformity as key factors influencing tensile strength estimates, with errors reflecting the *12* to *17%* variations in stiffness modulus observed here for contact angles of *10* to *30*° [29]. Recent FEM analyses by Guerrero-Miguel *et al.* [38] further corroborate anisotropy along vertical and horizontal radii, emphasizing platen stiffness effects that amplify uncertainties in compliant materials like bituminous mixtures. Mezouara *et al.* [19] quantified repeatability as contributing to *80%* of total uncertainty, consistent with our metrological interpretation where load profile discrepancies introduce systematic biases in LVDT-derived deformations.

Although indirect tensile tests (IT-CY) are standardized by EN 12697-26 [8] and ASTM D7012-23 [3], these protocols generally overlook the influence of load non-uniformity at the specimen–platen interface. The present numerical evidence demonstrates that assuming a uniform load profile leads to significant systematic errors in stiffness modulus estimation, primarily due to excessive stress concentrations reaching up to *40 MPa* in the vicinity of the contact zone. Furthermore, neglecting interface friction and pressure gradients artificially constrains transverse deformation near the specimen ends, resulting in a systematic overestimation of Poisson's ratio at the center of the cylinder [21-26].

The calculated error indicators reveal substantial stress discrepancies in the immediate contact region $\left(r / R < 0.20\right)$ between different load distribution models, confirming that the contact assumption is far from neutral. These numerical heterogeneities are consistent with experimental validations reported in the literature using digital image correlation (DIC) techniques [22], which highlight the occurrence of initial nonlinear responses induced by imperfect contact conditions.

From a metrological standpoint, these findings emphasize the necessity of refined contact modeling within existing standards [3, 8]. Failure to account for load non-uniformity may lead to an underestimation of the stiffness modulus and a concurrent overestimation of Poisson's ratio, thereby introducing systematic bias into material characterization. On a practical level, such inaccuracies directly affect pavement design calculations, potentially resulting in overestimated fatigue life predictions and reduced reliability of performance assessments [9, 10]. In high-precision applications, such as nanometrology or optical

measurements, localized stresses could induce sensor artifacts, increasing uncertainty in dimensional evaluations [41, 42].

In terms of metrological perspectives, to improve measurement precision and overcome identified sources of uncertainties–such as interface friction, platen misalignment, and non-uniform load distributions–it is conceivable to adopt integrated approaches on the basis of the Guide to the Expression of Uncertainty in Measurement (GUM) [43], including Monte Carlo simulations for robust quantification of combined uncertainty. For example, dynamic calibration of measurement devices, incorporating standards traceable to international norms (such as those from the BIPM), would allow quantification and correction of systematic biases related to mechanical play in platens, thereby reducing repeatability errors that account for up to 80% of total uncertainty [19]. The incorporation of non-contact measurement methods, such as digital image correlation (DIC) [22], could replace traditional LVDT sensors, avoiding slippage and local alterations in mechanical behavior, and offering sub-micrometric resolution to map heterogeneous deformations in real time. Additionally, global sensitivity analyses, combined with Monte Carlo simulations, would enable evaluation of uncertainty propagation related to geometric parameters (surface roughness, ovalization) and contact conditions, in alignment with the recommendations of ISO/IEC Guide 98-3 [44]. These metrological advances, applied to IT-CY tests, would promote optimization of experimental protocols, such as adaptive adjustment of contact angles or the use of variable-stiffness platens, to minimize artifacts and enhance traceability of stiffness modulus measurements, thereby contributing to a more reliable evaluation of bituminous mixture performance in road infrastructures.

On a practical level, the identified sensitivity of the stiffness modulus to load distribution profiles has direct implications for pavement engineering. The stiffness modulus (E) is a fundamental input parameter in fatigue life prediction models, such as: $\left(N_f = f\left(\varepsilon_t, E\right)\right)$. Where the number of cycles to failure $\left(N_f\right)$ strongly depends on the tensile strain $\left(\varepsilon_t\right)$ [45, 46, 47].

The numerical results of the present study indicate that assuming a uniform load distribution may lead to a significant error in the determination of the stiffness modulus. In a pavement design context, an underestimation of the modulus results in higher calculated tensile strains, which may lead to an erroneous prediction of a reduced fatigue life, and consequently to overdesigned structures or premature and costly maintenance interventions.

The limitations include the assumption of elastic behavior, omitting the viscoelasticity of bituminous mixtures, and the fixed contact angle; future investigations should incorporate time-dependent models (for example, via Prony series in Abaqus) and experimental validation through digital image correlation (DIC) [22], probabilistic sensitivity analyses [20] to more precisely quantify uncertainty propagation, optimizing protocols for sustainable infrastructure.

4. Conclusion

This finite element analysis, performed using Abaqus software, highlights the crucial role of load distribution profiles–uniform, sinusoidal, and parabolic–in modulating stress fields and the associated uncertainty in the stiffness modulus during indirect tensile tests on cylindrical specimens (IT-CY) of the material, with a fixed contact angle of *15*°. The simulations reveal significant variations: uniform loading generates pronounced stress heterogeneity, with radial peaks reaching up to *40 MPa* near the contact zones and discrepancies in circumferential stresses (hoop stress) exceeding *60%* compared to smoother profiles. These concentrations, resulting from abrupt transitions at the platen-specimen interface, thereby influencing the determination of the material's stiffness modulus. In contrast, sinusoidal and parabolic distributions promote progressive stress dissipation, reducing overall peaks by up to *60%* and confining high values along the vertical diameter, while keeping shear stresses at secondary levels (*20* to *25%* of radial components).
These results emphasize the need for refined modeling of contact conditions in standards such as EN 12697-26 [8] and ASTM D7012-23 [3], where neglecting non-uniformity can lead to an underestimation of the stiffness modulus and an overestimation of Poisson's ratio.

Although the study relies on the assumption of linear elastic behavior, omitting the inherent viscoelasticity of the material, and on a fixed contact angle, it identifies key limitations that could be mitigated in future work. These should incorporate time-dependent viscoelastic models, such as Prony series in Abaqus, to capture relaxation and creep effects, as well as experimental validation through digital image correlation (DIC) or high-speed imaging to map heterogeneous deformations in real time and corroborate numerical simulations. Optimizing test protocols via advanced metrological approaches, including uncertainty quantification according to the GUM [43], will enable more precise mechanical characterization of bituminous materials, contributing to more sustainable and reliable civil engineering practices.

Nomenclature

ASTM – American Society for Testing Materials.
BIPM – International Bureau of Weights and Measures.
D – diameter (mm)
E – stiffness modulus determined through measurements (MPa).
GUM – Guide to the Measurement of Uncertainty.
LVDT – Linear Variable Differential Transformer.
P – represents the total applied load, equivalent to that in the concentrated load scenario.
$P_0 = P / w$ – is the normalized load, obtained by dividing the total load by t specimen's thickness w.
R – is the radius of the disc,
t – average thickness of the specimen (mm).
α – represents the rotation angle from the vertical diameter to the line of action of the load,
δ – forced displacement of (μm)
ϑ – Poisson's coefficient.
ω_0 – represents the contact angle between the loading jaw and the specimen,

References

[1] Kumar S., Mukhopadhyay T., Waseem S., Singh B. and Iqbal M. (2016): *Effect of platen restraint on stress–strain behavior of concrete under uniaxial compression: a comparative study*.– Strength of Materials, vol.48, No.6, pp.832-841, https://doi.org/10.1007/s11223-016-9802-z.

[2] ASTM C39/39M-21 (2021): *Standard test method for compressive strength of cylindrical concrete specimens*.– ASTM International, West Conshohocken, PA, USA, https://doi.org/10.1520/C0039_C0039M-21.

[3] ASTM D7012-23 (2023): *Standard test method for compressive strength and elastic moduli of intact rock core specimens under varying states of stress and temperatures*.– ASTM International, West Conshohocken, PA, USA, vol.04.09, pp.1-10, https://doi.org/10.1520/D7012-23.

[4] ASTM D4543-19 (2019): *Standard practices for preparing rock core as cylindrical test specimens and verifying conformance to dimensional and shape tolerances*.– ASTM International, West Conshohocken, PA, USA, https://doi.org/10.1520/D4543-19.

[5] Peng J., Wong L.N.Y. and Teh C.I. (2018): *A re-examination of slenderness ratio effect on rock strength: insights from DEM grain-based modelling*.– Engineering Geology, vol.246, pp.245-254, https://doi.org/10.1016/j.enggeo.2018.10.003.

[6] Talaat A., Emad A., Tarek A., Masbouba M., Essam A. and Kohail M. (2021): *Factors affecting the results of concrete compression testing: a review*.– Ain Shams Engineering Journal, vol.12, No.1, pp.205-221, https://doi.org/10.1016/j.asej.2020.07.015.

[7] Alejano L.R., Arzúa J., Estévez-Ventosa X. and Suikkanen J. (2020): *Correcting indirect strain measurements in laboratory uniaxial compressive testing at various scales*.– Bulletin of Engineering Geology and the Environment, vol.79, No.9, pp.4975-4997, https://doi.org/10.1007/s10064-020-01853-4.

[8] European Standards EN 12697-26 (2007): *Bituminous mixtures – Test methods for hot mix asphalt. Part 26: Stiffness*.– Brussels: European Standards, https://standards.iteh.ai/catalog/standards/cen/49dbfc73-c6ec-4ba3-8b74-1bf1682782e4/en-12697-26-2004.

[9] Barman M., Ghabchi R., Singh D., Zaman M. and Commuri S. (2018): *An alternative analysis of indirect tensile test results for evaluating fatigue characteristics of asphalt mixes*.– Construction and Building Materials, vol.166, pp.204-213, https://doi.org/10.1016/j.conbuildmat.2018.01.049.

[10] Bennert T., Haas E. and Wass E. (2018): *Indirect tensile test (IDT) to determine asphalt mixture performance indicators during quality control testing in New Jersey*.– Transportation Research Record, vol.2672, No.28, pp.394-403, https://doi.org/10.1177/0361198118793276.

[11] Zhao Y., Jiang L., Jiang J. and Ni F. (2020): *Accuracy improvement for two-dimensional finite-element modeling while considering asphalt mixture meso-structure characteristics in indirect tensile test simulation*.– Journal of Materials in Civil Engineering, vol.32, No.11, p.04020275, https://doi.org/10.1061/(ASCE)MT.1943-5533.0003359.

[12] Zieliński P. (2020): *Indirect tensile test as a simple method for rut resistance evaluation of asphalt mixtures – Polish experience*.– Road Materials and Pavement Design, vol.23, No.3, pp.712-723, https://doi.org/10.1080/14680629.2020.1820894.

[13] Huang Z., Zhang Y., Li Y., Zhang D., Yang T. and Sui Z. (2021): *Determining tensile strength of rock by the direct tensile, Brazilian splitting, and three-point bending methods: a comparative study*.– Advances in Civil Engineering, vol.2021, p.5519230, https://doi.org/10.1155/2021/5519230.

[14] Fu J., Liu J., Zhang X., Lei L., Ma X. and Liu Z. (2017): *Mesoscale experimental procedure and finite element analysis for an indirect tensile test of asphalt concrete*.– Road Materials and Pavement Design, vol.19, No.8, pp.1906-1927, https://doi.org/10.1080/14680629.2017.1373142.

[15] Huang J., Duan T., Sun Y., Wang L. and Lei Y. (2020): *Finite element (FE) modeling of indirect tension to cylindrical (IT-CY) specimen test for damping asphalt mixtures (DAMs)*.– Advances in Civil Engineering, vol.2020, p.6694180, https://doi.org/10.1155/2020/6694180.

[16] Liu W., Gao Y. and Li L. (2018): *Micromechanical simulation of influence factors of indirect tensile test of asphalt mixture*.– Journal of Testing and Evaluation, vol.46, No.2, pp.832-841, https://doi.org/10.1520/JTE20160352.

[17] Peng Y., Wan L. and Sun L. (2017): *Three-dimensional discrete element modelling of influence factors of indirect tensile strength of asphalt mixtures*.– International Journal of Pavement Engineering, vol.20, No.11, pp.1306-1315, https://doi.org/10.1080/10298436.2017.1334459.

[18] Wu N., Fu J., Zhu Z. and Sun B. (2020): *Experimental study on the dynamic behavior of the Brazilian disc sample of rock material*.– International Journal of Rock Mechanics and Mining Sciences, vol.130, p.104326, https://doi.org/10.1016/j.ijrmms.2020.104326.

[19] Mezouara H., Zniker H., Feddal I., El Kouifat M.K. and El Hasnaoui M. (2025): *Sensitivity analysis and uncertainty quantification of stiffness modulus using indirect tensile test*.– International Journal of Applied Mechanics and Engineering, vol.30, No.2, pp.105-123, https://doi.org/10.59441/ijame/203165.

[20] Keaveny T.M., Pinilla T.P., Crawford R.P., Kopperdahl D.L. and Lou A. (1997): *Systematic and random errors in compression testing of trabecular bone*.– Journal of Orthopaedic Research, vol.15, No.1, pp.101-110, https://doi.org/10.1002/jor.1100150115.

[21] Marter A.D., Dickinson A.S., Pierron F. and Browne M. (2018): *A practical procedure for measuring the stiffness of foam-like materials*.– Experimental Techniques, vol.42, No.4, pp.439-452, https://doi.org/10.1007/s40799-018-0247-0.

[22] Crammond G., Boyd S.W. and Dulieu-Barton J.M. (2013): *Speckle pattern quality assessment for digital image correlation*.– Optics and Lasers in Engineering, vol.51, No.12, pp.1368-1378, https://doi.org/10.1016/j.optlaseng.2013.03.014.

[23] Markides Ch.F. and Kourkoulis S.K. (2012): *The stress field in a standardized Brazilian disc: the influence of the loading type acting on the actual contact length*.– Rock Mechanics and Rock Engineering, vol.45, No.2, pp.145-158, https://doi.org/10.1007/s00603-011-0201-2.

[24] Lavrov A. and Vervoort A. (2002): *Theoretical treatment of tangential loading effects on the Brazilian test stress distribution*.– International Journal of Rock Mechanics and Mining Sciences, vol.39, No.2, pp.275-283, https://doi.org/10.1016/S1365-1609(02)00010-2.

[25] Yuan R. and Shen B. (2017): *Numerical modelling of the contact condition of a Brazilian disk test and its influence on the tensile strength of rock*.– International Journal of Rock Mechanics and Mining Sciences, vol.93, pp.54-65, https://doi.org/10.1016/j.ijrmms.2017.01.010.

[26] Kostic S., Miljojkovic J., Simunovic G., Vukelic D. and Tadic B. (2022): *Uncertainty in the determination of elastic modulus by tensile testing*.– Engineering Science and Technology, an International Journal, vol.25, p.100998, https://doi.org/10.1016/j.jestch.2021.05.002

[27] Japaridze L. (2015): *Stress-deformed state of cylindrical specimens during indirect tensile strength testing*.– J. of Rock Mechanics and Geotechnical Eng., vol.7, No.5, pp.509-518, https://doi.org/10.1016/j.jrmge.2015.06.006.

[28] Liao Z.Y., Zhu J.B. and Tang C.A. (2019): *Numerical investigation of rock tensile strength determined by direct tension, Brazilian and three-point bending tests*.– International Journal of Rock Mechanics and Mining Sciences, vol.115, pp.21-32, https://doi.org/10.1016/j.ijrmms.2019.01.007.

[29] Yu J., Shang X. and Wu P. (2019): *Influence of pressure distribution and friction on determining mechanical properties in the Brazilian test: theory and experiment*.– International Journal of Solids and Structures, vol.161, pp.11-22, https://doi.org/10.1016/j.ijsolstr.2018.11.002.

[30] Kourkoulis S.K., Markides Ch.F. and Chatzistergos P.E. (2013): *The standardized Brazilian disc test as a contact problem*.– International Journal of Rock Mechanics and Mining Sciences, vol.57, pp.132-141, https://doi.org/10.1016/j.ijrmms.2012.07.016.

[31] Yu Y., Zhang J. and Zhang J. (2009): *A modified Brazilian disk tension test*.– International Journal of Rock Mechanics and Mining Sciences, vol.46, No.2, pp.421-425, https://doi.org/10.1016/j.ijrmms.2008.04.008.

[32] Erarslan N. and Williams D.J. (2012): *Experimental, numerical and analytical studies on tensile strength of rocks*.– Int. J. of Rock Mechanics and Mining Sciences, vol.49, pp.21-30, https://doi.org/10.1016/j.ijrmms.2011.11.007.

[33] Markides Ch.F. and Kourkoulis S.K. (2016): *The influence of jaw's curvature on the results of the Brazilian disc test*.– J. of Rock Mechanics and Geotechnical Eng., vol.8, No.2, pp.127-146, https://doi.org/10.1016/j.jrmge.2015.09.008.

[34] Komurlu E. and Kesimal A. (2015): *Evaluation of indirect tensile strength of rocks using different types of jaws*.– Rock Mechanics and Rock Engineering, vol.48, No.4, pp.1723-1730, https://doi.org/10.1007/s00603-014-0644-3.

[35] Gutiérrez-Moizant R., Ramírez-Berasategui M., Santos-Cuadros S and García-Fernández C.C. (2020): *A novel analytical solution for the Brazilian test with loading arcs*.– Mathematical Problems in Engineering, vol.2020, p.2935812, https://doi.org/10.1155/2020/2935812.

[36] Li D. and Wong L. (2012): *The Brazilian disc test for rock mechanics applications: review and new insights*.– Rock Mechanics and Rock Engineering, vol.46, No.2, pp.269-287, https://doi.org/10.1007/s00603-012-0257-7.

[37] Huang Y.G., Wang L.G., Lu Y.L., Chen J.R. and Zhang J.H. (2015): *Semi-analytical and numerical studies on the flattened Brazilian splitting test used for measuring the indirect tensile strength of rocks*.– Rock Mechanics and Rock Engineering, vol.48, No.5, pp.1849-1866, https://doi.org/10.1007/s00603-014-0676-8.

[38] Guerrero-Miguel D.J., Álvarez-Fernández M.I., Ramírez-Berasategui M., Prendes-Gero M.B. and González-Nicieza C. (2024): *Influence of platen stiffness on the contact stress distribution in the standardized uniaxial compression test*.– Mathematics, vol.12, No.13, p.1943, https://doi.org/10.3390/math12131943.

[39] Garcia-Fernandez C.C., Gonzalez-Nicieza C., Alvarez-Fernandez M.I. and Gutierrez-Moizant R.A. (2018): *Analytical and experimental study of failure onset during a Brazilian test*.– International Journal of Rock Mechanics and Mining Sciences, vol.103, pp.254-265, https://doi.org/10.1016/j.ijrmms.2018.01.045.

[40] García V.J., Márquez C.O., Zúñiga-Suárez A.R., Zuñiga-Torres B.C. and Villalta-Granda L.J. (2017): *Brazilian test of concrete specimens subjected to different loading geometries: review and new insights*.– International Journal of Concrete Structures and Materials, vol.11, No.2, pp.343-363, https://doi.org/10.1007/s40069-017-0194-7.

[41] Cagliero R., Barbato G., Maizza G. and Genta G. (2015): *Measurement of elastic modulus by instrumented indentation in the macro-range: uncertainty evaluation*.– International Journal of Mechanical Sciences, vol.101-102, pp.161-169, https://doi.org/10.1016/j.ijmecsci.2015.07.030.

[42] Suttner S. and Merklein M. (2017): *A new approach for the determination of the linear elastic modulus from uniaxial tensile tests of sheet metals*.– Journal of Materials Processing Technology, vol.241, pp.64-72, https://doi.org/10.1016/j.jmatprotec.2016.10.024.

[43] BIPM, IEC, IFCC, ILAC, ISO, IUPAC, IUPAP and OIML (2008): *Evaluation of measurement data – Guide to the expression of uncertainty in measurement*.– Joint Committee for Guides in Metrology, JCGM 100:2008, https://doi.org/10.59161/JCGM100-2008E.

[44] ISO/IEC Guide 98-3 (2008): *Uncertainty of Measurement – Part 3: Guide to the expression of uncertainty in measurement (GUM:1995)*.– Geneva: International Organization for Standardization, https://www.iso.org/standard/50465.html.

[45] Zhou F. and Fernando E. (2007): *A Review of Performance Models and Test Procedures with Recommendations for Use in the Texas M-E Design Program*.– Texas Transportation Institute, College Station, TX, USA, Report Project 0-5798, https://static.tti.tamu.edu/tti.tamu.edu/documents/0-5798-1.pdf.

[46] Harnaeni S.R., Sunarjono S., Maghfirona A., Larasati V.P., Tanoedji Z.N., Ibrahim H.I. and Ayob A. (2025): *Flexible pavement remaining life due to elastic modulus decrease based on the Bina Marga 2017 method and the Asphalt Institute method*.– J. of Applied Eng. Science, vol.23, No.3, pp.631-646, https://doi.org/10.5937/jaes0-55496.

[47] Zbiciak A., Brzeziński K. and Wesołowski M. (2025): *Fuzzy-modulus-based layered elastic analysis of asphalt pavements for enhanced fatigue life prediction*.– Materials, vol.18, No.13, p.3034, https://doi.org/10.3390/ma18133034.

Received: November 2, 2025
Revised: May 4, 2026